A Review on Simplified Image Analysis Method for Measuring LNAPL Saturation Under Groundwater Table Fluctuation

Doaa F. Almaliki and Harris Ramli

Abstract The leaking from surface spills and underground storage tanks of various light non-aqueous phase liquids (LNAPLs) caused hazardous contamination to the subsurface system, especially in case of groundwater table fluctuations. The toxicity of these compounds has made infeasible field studies and gets a replacement with laboratory studies. Researchers have recently become very interested in using image analysis techniques to measure the saturation migration of groundwater and LNAPLs. Over the last decade, the simplified image analysis method (SIAM) has become increasingly popular. SIAM has been proved to be a suitable and effective tool for characterization and measuring LNAPL migration in the subsurface system. This research introduces a review of the recent studies and published on the simplified image analysis method for LNAPL migration measurements. The experimental approaches in this study can be viewed as an important intermediary between column studies and tank studies. Besides discussion on the research efforts, recommendations for future research are provided.

Keywords Groundwater fluctuation · Saturation · LNAPL · Hazardous waste · SIAM

D. F. Almaliki · H. Ramli (✉)
School of Civil Engineering, Engineering Campus, Universiti Sains Malaysia, 14300 Nibong Tebal, Pulau Pinang, Malaysia
e-mail: cemhr@usm.my

D. F. Almaliki
e-mail: doaa.faisal@stu.edu.iq

D. F. Almaliki
Environment and Pollution Engineering Department, Basrah Engineering Technical College, Southern Technical University, Alzybair Street, Basrah, Iraq

© The Author(s), under exclusive license to Springer Nature Singapore Pte Ltd. 2024

N. Sabtu (ed.), *Proceedings of AWAM International Conference on Civil Engineering 2022 - Volume 3*, Lecture Notes in Civil Engineering 386,
https://doi.org/10.1007/978-981-99-6026-2_8

1 Introduction

The release of petroleum hydrocarbon liquids is a worldwide phenomenon that has been increasing in conjunction with rising oil consumption [1]. Rapid global population expansion [2], industrialization, and modern transportation have all increased demand for oil, increasing oil spills. An example of an oil incident that released oil between (2,100,000 and 2,400,000 barrels) is the Canada Atlantic Empress oil spill [3]. Pipeline ruptures, vandalism, human error, system failures, [4] collisions, and shipwrecks are the most common causes of oil spills. Crude oil spill expenses, cleaning costs, and rehabilitation costs are all examples of catastrophic economic and environmental disasters [5].

Environmental impacts of hydrocarbon product spills include water pollution (surface and groundwater) [6], seashore, and beach contamination [7]. Degradation of marine invertebrate habitat, individual oiling, and drowning, alteration of the food chain and toxicity [8, 9], mortality, and killing the marine birds [10–12] has all been identified. There has also been a decline in vegetation and marine mammals [13–15]. The slow response to oil leak disasters aggravates the severity of these risks. Fast reaction to oil spillage reduces its migration and lowers the potential effects [16–19].

Groundwater is an important element for humans. There is a significant need to reduce contaminated groundwater and use it as a source of drinking water in the future. Petroleum fuels are contaminating groundwater all over the world due to leakage from the underground storage tanks, leaking pipes, and unintentional spills. When these products are released on the ground, they migrate downward until reaching the water table. An example of petroleum fuels is the light non-aqueous phase liquids (LNAPLs). The LNAPLs cause reduction in the elevation of the water saturation if the spilled volume of LNAPL is high [20].

From previous LNAPL research to the current knowledge, there have been substantial improvements. The researchers provide that LNAPL is variably saturated in the underground system where the LNAPL can exist in free (mobile), entrapped, and residual forms. Understanding all the types of LNAPL distribution in the subsurface is essential for establishing a successful LNAPL remediation approach [21] as well as assessing the potential for environmental and human health harm [22].

Chevalier and Petersen [23] conducted an earlier literature evaluation of LNAPL flow, transport, and remedial techniques in 2D laboratory aquifer models. Later, Saleem et al. [24] investigated direct and indirect techniques for determining spilled hydrocarbon volume utilizing state-of-the-art technology. The authors in their research emphasized the significance of interdisciplinary collaboration between scientists and engineers. A review of multidimensional, multi-fluid, intermediate-scale experiments was demonstrated by Oostrom et al. [25]. Experimental aspects of LNAPL dissolution and increased remediation are covered in their review. The authors also studied the behavior of groundwater flow, saturation imaging techniques, and tracer detection in 2D laboratory experiments [26]. Recently, a critical review paper discussed the effect of ecohydrology, and ecohydrological interface on heavy

metals and organic pollutants. It focused on the indispensable role of the ecohydrological interface in the removal of pollutants [27]. Another critical review focused on only two factors which are the ground-level fluctuation and the change in temperature and how it affects LNAPL spreading and degradation processes [28].

Many researchers used image analysis techniques to study the saturation distribution of groundwater and LNAPL in the subsurface system. Such methods are, the multispectral image analysis method (MIAM), light transmission visualization (LTV), ground penetration radar (GPR), and light reflection method (LRM). The widespread use of image analysis methods in a variety of research domains demonstrates that these methods are quite beneficial, particularly for examining the behavior of complicated types of pollutants and determining saturation. However, there is a lack of review papers on the investigation of groundwater and LNAPL using the simplified image analysis method. Therefore, this study will focus on using the simplified image analysis method to measure the saturation distribution of groundwater and LNAPL in the whole domain under fluctuated groundwater table. The next subjects will examine a general overview of groundwater movement and contamination by LNAPL as well as describe the main design of SIAM and some related studies that took into account this technique to measure the groundwater contamination saturation.

2 LNAPL Contamination on Subsurface

2.1 LNAPL Migration Behavior in the Subsurface

Light non-aqueous phase liquid (LNAPL) refers to the petroleum hydrocarbons liquid that is lighter than water. It is a type of groundwater constituent that has a lower density than water and is sparingly soluble. When LNAPL is released on the ground, it moves through the unsaturated zone before accumulating in the saturated zone. Capillary pressures produce a drop in the water percentage in the capillary fringe by keeping a residual fraction of the contaminant in the pore space during migration (see Fig. 1) [29–32]. The distribution of LNAPL in the subsurface during infiltration is complicated and varies on various parameters [33]. Dissolved and gaseous phases of LNAPL are commonly found in the ground as by-products of the pure phase. As a result, these various phases interact with the soil–water system, creating a variety of chemical and physical changes in the soil [34].

Several factors influence the migration of LNAPL in the subsurface, including the volume of NAPL released, the duration of the release, the surface of the infiltration, soil characteristics, the properties of LNAPL, and the subsurface flow conditions [35]. When LNAPL is released into the subsurface, it migrates down through the unsaturated zone as a separate liquid due to gravity's action. The vertical movement of the contaminant is accompanied by horizontal migration. This is attributed to the medium spatial variability and capillary forces effect [36]. During LNAPL

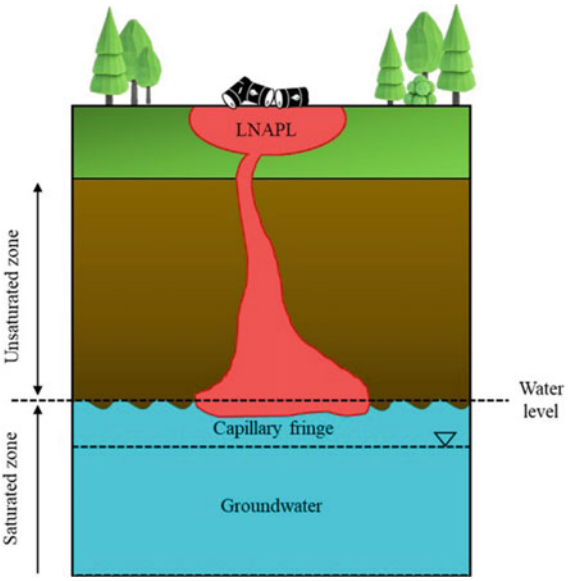

Fig. 1 LNAPL migration in the subsurface system [22]

vertical migration in the unsaturated zone, the residual liquid is trapped in pore spaces. Because of the surface tension effects, this trapping occurs. Some LNAPL will eventually reach the saturated zone where it will propagate horizontally through the capillary fringe when sufficient LNAPL volume is released [36].

2.2 Effect of Groundwater Fluctuation on the Distribution of LNAPL

Groundwater table variations can alter the distribution of the multiple LNAPL phases in the subsurface. Free LNAPL may become entrapped or entrapped LNAPL may become free LNAPL as the water table rises or decreases. Furthermore, as the groundwater level declines during the dry season, free LNAPL may become a residual form in the unsaturated zone, as the majority of free LNAPL migrates downward with the water table [37].

Water table oscillations may have a significant impact on LNAPL redistribution, mobility, and phase partitioning. Several in situ cleanup techniques rely on pollutant behavior within porous media. The chemical and the physical traits of the contaminants, the chemistry of the subsurface environment, the flow rate of groundwater, and other hydraulic characteristics are all factors that influence the water table fluctuation in the real world [38]. Most of the researchers concentrate on the dispersion and distribution of contaminants in groundwater using horizontal flow systems, however,

there is still a little attention to the influence of the level of groundwater table on pollutants, where groundwater levels are unstable and fluctuate.

When the groundwater table drops, LNAPL follows, causing LNAPL redistribution and reformation of LNAPL components between phases. In the subsurface saturation zone, a portion of the LNAPL remains as discontinuous residual LNAPL ganglia. By successive water infiltration, the LNAPL's most volatile and soluble chemicals can volatilize or be leached, contributing to the dissolved plume's evolution. Mobile LNAPL is redistributed higher as the water table rises, leaving some immobile entrapped LNAPL droplets in the saturated zone [39–43].

During repeated drainage/imbibition phases, the influence of capillary pressure, as well as the trapping of fluids in the saturated and unsaturated zones, continuously changes the water flow paths [44]. Additional interactions between LNAPL and water (rainwater and groundwater) improve hysteresis effects, promoting the migration of pollutants (see Fig. 2) [45, 46]. As a result, seasonal or pump-induced groundwater level fluctuations commonly cause major pollution dispersion and redistribution through the water table fluctuation zone. It also lowers the average LNAPL saturation and mass of the mobile light NAPL that remains afterward.

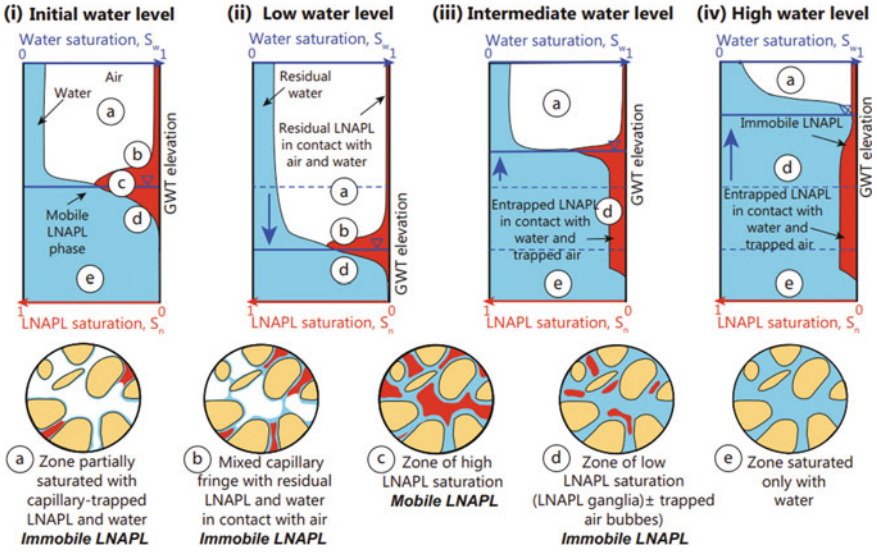

Fig. 2 Fluctuation of LNAPL (S_n) and water (S_w) saturation in soil under the influence of water table variations [47]

3 Simplified Image Analysis Method for Measuring Groundwater and LNAPL Saturation

Simplified image analysis method (SIAM) is a non-invasive and non-intrusive method for determining fluid saturations over a wide area. SIAM needs the least am out of equipment, is the cheapest, and produces no adverse radiation effects [48].

3.1 Design and Advantages of SIAM

Two types of digital cameras were used in the experiment using SIAM, which is Nikon D90 and Nikon D7000. Both of these digital cameras consist of two non-similar band-pass filters with wavelengths of 450 and 656 nm that are required to quantify the saturation distribution of LNAPL using SIAM. To collect photographs during the experiments, the cameras must be set in front of the experimental design (column or tank). As the only source of light in the dark room, two LED floodlights were placed. As a reference for white color, a GretagMacbeth white balance board was fixed next to the experimental design (see Fig. 3). Blue-dyed water (Brilliant blue FCF added to the solution at a 1:10,000 weight ratio) and red-dyed LNAPL were also used to enhance the visualization of LNAPL movement (Sudan III mixed with LNAPL Liquid at a 1:10,000 mass relation). The Nikon Camera Control Pro software was used to control the digital cameras to minimize displacement and vibrations. The aperture settings of the two lenses were modified using exposure periods of a few seconds to fully use the camera's dynamic range. The lenses' apertures were set to f-16 and the exposure length was 2.5 s for all of the photos. Nikon ViewNX 2.10.3 is required to convert all images from NEF (Nikon proprietary RAW version files) to Tagged Image File Format (TIFF). The TIFF images then are analyzed using MATLAB [49].

The theory that supports SIAM is the use of the Beer–Lambert equation of transmittance to develop a correlation between fluid saturations and average optical density, which can then be used to estimate fluid saturations of porous media across the entire experimental [48].

When a beam of monochromatic light I_o intersects with a block of absorbing matter perpendicular to a surface, its power is decreased to I_t as a result of absorption after traveling through a length b of the material, according to the Beer–Lambert law of transmittance:

$$D_i = \in bc = \log_{10} \frac{I_o}{I_t} \tag{1}$$

where D_i is the optical density, ε is the numerical constant, b is the length of the path, is the number of moles per liter of absorbing solution, I_o is the initial radiant power, and I_t is the transmitted power [50]. The average optical density (AOD) D_i

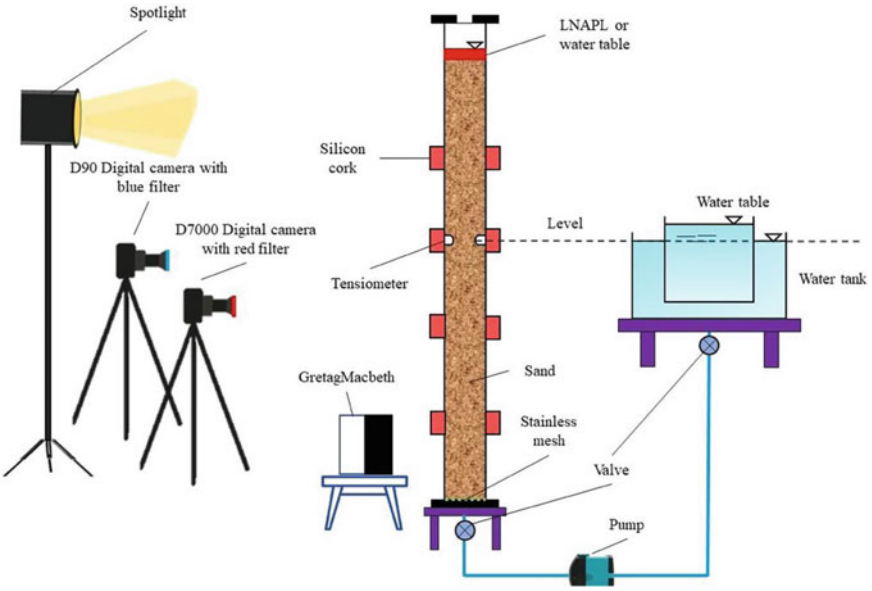

Fig. 3 Experimental setup [49]

for reflected light intensity in digital photographs is defined as:

$$D_i = \frac{1}{N}\sum_{j=1}^{N} d_{ji} = \frac{1}{N}\sum_{j=1}^{N}\left(-\log_{10}\left(\frac{I_{ji}^{r}}{I_{ji}^{0}}\right)\right) \tag{2}$$

From Eq. (2), a total number of pixels in the selected area is N, the optical density of the individual pixels for a given spectral band I is d_{ji}, I_{ji}^{r} is the reflected light intensity, as determined by individual pixel values, and I_{ji}^{0} is the intensity of reflected light using a brilliant white surface [51].

$$D_t = c.D_o \tag{3}$$

where D_0 is the optical density of a solution of unit concentration, and D_t is the optical density of a solution with a concentration of c. So, when two cameras with band-pass filters (wavelengths = I and j) are employed, and water and NAPL are combined with dyes whose predominant color wavelengths are both I and j, two sets of linear equations can be solved for S_w and S_o:

$$\left[\begin{pmatrix} D_i \\ D_j \end{pmatrix}_{m.n}\right] = \begin{bmatrix} \left(D_i^{10} - D_i^{00}\right).S^w + \left(D_i^{01} - D_i^{00}\right).S_o + D_i^{00} \\ \left(D_j^{10} - D_j^{00}\right).S^w + \left(D_j^{01} - D_j^{00}\right).S_o + D_j^{00} \end{bmatrix} \tag{4}$$

Table 1 Summary of SIAM technique design

Technique	Simplified image analysis method (SIAM)
Method application	Measuring LNAPL and water saturation distribution in 1D column
Average optical density (AOD)	The AOD equations are unique to each mesh element (matrix)
Number of cameras	2 cameras
Number of filters	2 filters (450 and 656 nm)
Calibrated sample	Experimental domain (column)
Experiment calibration	3 non-linear points were used to generate a linear regression plane from these images ($S_w = 0\%$ $S_o = 0\%$ dry sand $S_w = 100\%$ $S_o = 0\%$ sand fully saturated with water $S_w = 0\%$ $S_o = 100\%$ sand saturated with LNAPL)
Advantages	Measuring the saturation in the whole domain

$[D_j]_{mn}$ is the average optical density of each mesh element for wavelengths i and j; $\left[D_i^{00}\right]_{mn}$ and $\left[D_j^{00}\right]_{mn}$ represent the average optical density of each mesh element of dry sand; $\left[D_i^{10}\right]_{mn}$ and $\left[D_i^{10}\right]_{mn}$, water-saturated sand, and $\left[D_i^{01}\right]_{mn}$ and $\left[D_i^{01}\right]_{mn}$ for LNAPL-saturated sand [48].

This technique requires two cameras with two different band-pass filters (wavelengths $\lambda = i$ and j) to obtain three calibration photos. Each camera must be calibrated based on the photo of the studied domain filled with dry sand, water-saturated sand, and LNAPL-saturated sand. The average optical densities for each mesh element of the examined domain are analyzed and differentiated to the corresponding ones for all three cases, as well as a correlation matrix. The next section will propose to summarize current knowledge on measuring groundwater and LNAPL distribution underwater table fluctuation using SIAM (Table 1).

3.2 Measuring Groundwater and LNAPL Saturation Using SIAM

Several researchers conducted their studies on the migration of groundwater and LNAPL using SIAM. Flores et al. [48] had a novel study on the simplified image analysis method. The simplified image analysis method had been used for analyzing the behavior of the two-phase air–water and three-phase air–water-LNAPL fluctuating groundwater systems. Under dynamic conditions, the 1D column porous soil (Toyoura sand) contaminated with LNAPLs showed a 4.7% difference in the

drainage-imbibition three-phase air–water-LNAPL. Another study presented by Flores et al. [52] described the movement of LNAPL and groundwater in four drainage/imbibition cycles in a three-phase system in a 1D column containing fully saturated sand. At the same point of each step, the findings revealed distinct saturation levels, which improves the effect of the groundwater movement on the distribution of the water and the contaminant through rising and decreasing of the water table level. Similar research by Flores et al. [53] measured three-phase saturation of water and diesel in granular soil. SIAM was used to investigate the migration behavior of diesel in a 1D column filled with Toyoura sand under various precipitation conditions (6.6 and 63.2 mm/h). The study's findings revealed that the residual LNAPL saturation could be anticipated based on the maximum saturation. Further studies need to be done in a two-dimensional tank to measure the vertical and horizontal movements of LNAPL.

A one-dimensional column was used in conjunction with SIAM by Sudsaeng et al. [54]. They studied the migration of diesel in porous media under variable groundwater conditions. Toyoura sand and Silica #5 sand were used as porous media in this study. According to this study, diesel saturation is higher in Toyoura sand than in Silica #5 sand at the end of imbibition processes, and sand particle size has a major impact on diesel migration behavior. Water and LNAPL saturation distribution under the influence of groundwater fluctuation will be different in various sands, according to this study.

Only two published researches on the NAPL saturation migration in granular soil comparing different NAPLs with different densities and viscosity were explored by Flores et al. [55, 56]. The researchers established a logarithmic relationship between viscosity and residual saturation ratios of various NAPLs, which may be utilized to compute residual saturation values after imbibition. Even though LNAPLs has a lower density than water, their findings show that they can effectively be trapped below the water table. Flores et al. showed in the second investigation that the infiltrated LNAPL depth was significantly related to the viscosity of the pollutant (R^2 = 0.84). The variations in the depth of the LNAPL mobile fraction after both the drainage/imbibition steps were also directly related to interfacial tension values (R^2 = 0.79). The viscosity was also logarithmically connected to the residual saturation under the same conditions. The researches help to understand and anticipate the properties of various spilled contaminants on the ground.

In addition to studying the effect of density and viscosity of the contaminant on its migration, experiments on the influence of LNAPL volume on the contaminant migration were done by several researchers. The experiment was described by Alazaiza et al. [57] in laboratory 1D column tests. The effect of water infiltration on pooled light non-aqueous phase liquid (LNAPL) redistribution in porous media was investigated using SIAM. Low and high levels of LNAPL were determined in the experiments. The capillary fringe was found to be around 6–7 cm long, which corresponded to the capillary height calculated using empirical equations. This presented that LNAPL contamination migrated further into the capillary fringe zone when the volume of the contaminant was large. Also, it showed that injected water produced a greater hydrodynamic force on the entrapped LNAPL, causing it to move further

into the capillary and saturation zones. Similarly, another study done by Alazaiza et al. [58] in one-dimensional column experiments to show the effect of the volume of LNAPL on the migration of the contaminant was carried out to see how varying LNAPL volumes affected the behavior of LANPL distribution in the capillary zone in the system. Various three diesel volumes (50, 100, and 150) ml were used in separate experiments. The research demonstrated that the larger volume of diesel (150 ml) leads to faster LNAPL migration. This means that the higher injected volume, the faster migration of the contaminant deeper into the capillary fringe which contributes to the distinction of groundwater quality. SIAM also was used by Alazaiza et al. [59] to expose groundwater and LNAPL migration under the effect of two diesel volumes (low and high) and two patterns of water table fluctuation. When the water table drained, the water saturation decreased, however, the LNAPL saturation rose. By increasing the diesel volume from 25 to 50 ml, the initial saturation of diesel was raised above the groundwater table and the capillary fringe height extended from 36 to 38 cm. It is relatively clear when comparing the two LNAPL volumes, that it was discovered that the LNAPL in the case of high LNAPL covered a larger area. It seems, therefore, relatively clear that increasing LNAPL volume while keeping the same groundwater fluctuation pattern shows a slight influence on LNAPL's overall behavior.

The emphasis of the research by Harris [49, 60] was to assess diesel migratory behavior in the subsurface as a result of precipitation in one 1D column and 2D tank tests. The impact of precipitation intensity was considered. The study showed that the higher the intensity, the deeper the LNAPL will migrate into the saturated zone as a result of precipitation. S-p relationships can also be used to track potential LNAPL spills and migration as a function of precipitation, according to the study's findings. The author also concluded that diesel saturation was higher in the first drainage than in the second drainage, implying that some residual diesel was retained beneath the water table. The author's findings also reveal that in a 2D tank, the higher the horizontal groundwater flow, the bigger the diesel contamination. The displacement of the LNAPL in vertical groundwater movements might be upward or follow above the soil surface. Continuously, Sudsaeng et al. [61] have used SIAM to evaluate the impact of ground-water fluctuation on diesel distribution in the subsurface in a one-dimensional column. They also used a 2D tank experiment to investigate the impacts of groundwater table fluctuation and lateral groundwater flow. Their findings show that the greater the contaminated area by diesel, the large rate of horizontal groundwater movement. In the case of the vertical flow of groundwater, the LNAPL moves upward to the soil surface.

Yimsiri et al. [62] completed a one-dimensional column experiment, in which they focused on the impact of different particle sizes on the saturation of water and LNAPL in the main domain under transient conditions. Also, they investigated two-phase experimental data to show the soil-liquid characteristic curves (SLCCs) of diesel/air and water/air systems. Scaling procedures were used to estimate the soil liquids characteristic curve of the diesel/water system. The authors showed that smaller particle sizes affect the distribution of the contamination. They cause lower pressure entrance, residual matric suction, and residual saturation degree. The coarser

Table 2 Summary of experimental research used SIAM

Ref	LNAPL type	Soil type	LNAPL volume	Design dimension	Software
[48]	Paraffin	Toyoura sand	28 g	1D (3.5 × 3.5 × 50) cm	MATLAB
[52]	Paraffin	Toyoura sand	13.8 g	1D (3.5 × 3.5 × 60) cm	MATLAB
[53]	Diesel	Toyoura sand	/	1D (3.5 × 3.5 × 50) cm	MATLAB
[54]	Diesel	Toyoura sand, silica #5	28 g	1D (3.5 × 3.5 × 50) cm	MATLAB
[55]	10 NAPL	Granular soils Toyoura sand	50 ml	1D (3.5 × 3.5 × 40) cm	MATLAB
[56]	10 NAPL	Toyoura sand	50 ml	1D (3.5 × 3.5 × 50) cm	MATLAB
[57]	Diesel	River sand	(25, 50) ml	1D (35 × 35 × 600) mm	MATLAB
[58]	Diesel	River sand	(50, 100, 150) ml	1D (30 × 30 × 500) mm	MATLAB
[59]	Diesel	River sand	(25, 50) ml	1D (35 × 35 × 600) mm	MATLAB
[49]	Diesel	Toyoura sand	(25, 50) ml	1D (35 × 35 × 500) mm, 2D(500 × 700 × 35) mm	MATLAB
[60]	Diesel	River sand, Toyoura sand	(25, 50) ml	1D (35 × 35 × 600) mm	MATLAB
[61]	Diesel	Toyoura sand	(1D = 28 g), (2D = 300 g)	1D (3.5 × 3.5 × 50) cm, 2D (80 × 50 × 7.5) cm	MATLAB
[62]	Diesel	Ottawa sand (#3821, #3820)	15 g	1D (3.5 × 3.5 × 110) cm	MATLAB
[63]	0	Quarry sand	0	1D (35 × 35 × 550) mm	MATLAB

particle size results in lower entrapped LNAPL saturation and increase the entrapped air saturation. Another study related to the effect of particle size on the migration of LNAPL under water table fluctuation was done by Harris et al. [63]. They emphasized using the SIAM to estimate water saturation and capillary rise to get the grain shape constant. The study included six one-dimensional columns were used to model capillary rise at constant groundwater levels. The findings of this study showed that coarser sand should be measured with values less than 25 mm^2, whereas finer sand should be measured with values greater than 25 mm^2. Table 2 gives a summary of LNAPL migration studies done by using SIAM.

4 Conclusion

This review evaluates the use of the simplified image analysis method (SIAM) for measuring the LNAPL and groundwater migration in the subsurface system under the influence of groundwater table fluctuation. As several researchers prefer doing their studies using non-destructive and non-intrusive techniques like the simplified image

analysis method, using developed digital cameras, up-to-date toolbox like Image-Pro Plus software, and a new version of MATLAB is the best choice for image processing. The review concludes that SIAM is a good method in terms of groundwater contamination saturation measurements. It is a cost-effective method that doesn't require a lot of equipment, as well as it measures the contaminant saturation in the whole domain.

Studying the effect of groundwater fluctuation is still complex and often limited. According to worldwide predictions, the higher the groundwater table variations, the higher the LNAPL mobility. Higher precipitation and groundwater levels may cause the LNAPL compounds to be diluted and submerged in groundwater and connected streams. Groundwater table fluctuations in all studies show high influence on the migration of LNAPL in the system. The studies showed that the contaminant moves with the movement of the water table producing trapped and residual contaminants in the study region. The amplitude of LNAPL may influence the concentration of dissolved LNAPL and the moisture content of the soil.

Also, this paper shows that there are quite very few studies dealing with measuring the water and contaminant distribution in the subsurface system using a two-dimensional tank experiment, need, therefore, to be considered to study the movement behavior of the contaminant in term of groundwater fluctuations. Moreover, there is still a deficiency in the effect of both LNAPL and variation in the water table in conjunction with the particle size distribution in the main domain. Soil permeability is one of the key elements that determine the migration path and rainwater infiltration. It depends on the soil grain sizes and composition. The distribution of light non-aqueous phase liquid in layered homogeneous sand is still not covered by the simplified image analysis method. Furthermore, there are also very few studies that examined the effects of density and viscosity on the movement of the contaminant in the whole domain. For these issues, the complexity of LNAPL chemical, soil composition, and heterogeneity, and the groundwater table fluctuations amplitude in terms of groundwater table fluctuation needs to be studied. Finally, future laboratory simulations should take into account the most current technological advances in this field.

References

1. Chen, J., Zhang, W., Wan, Z., Li, S., Huang, T., Fei, Y.: Oil spills from global tankers: status review and future governance. J. Clean. Prod. **227**, 20–32 (2019)
2. Yekeen, S., Balogun, A., Aina, Y.: Early warning systems and geospatial tools: managing disasters for urban sustainability. In: Sustainable Cities and Communities, pp. 1–13. Springer International Publishing, Cham, Switzerland (2019)
3. Michel, J., Fingas, M.: Oil spills: causes, consequences, prevention, and countermeasures. In: Fossil Fuels. Research Planning, Inc., Columbia, SC, USA (2015)
4. Pelta, R., Carmon, N., Ben-Dor, E.: A machine learning approach to detect crude oil contamination in a real scenario using hyperspectral remote sensing. Int. J. Appl. Earth Obs. Geoinf. **82**, 101901 (2019)

5. Jiao, Z., Jia, G., Cai, Y.: A new approach to oil spill detection that combines deep learning with unmanned aerial vehicles. Comput. Ind. Eng. **135**, 1300–1311 (2019)
6. Nwachukwu, A.N., Osuagwu, J.C.: Effects of oil spillage on groundwater quality in Nigeria. Am. J. Eng. Res. AJER **3**, 271–274 (2014)
7. Mignucci-Giannoni, A.: Assessment and rehabilitation of wildlife affected by an oil spill in Puerto Rico. Environ. Pollut. **104**, 323–333 (1999)
8. Fingas, M.: The Basics of Oil Spill Cleanup. CRC Press, Boca Raton, FL, USA (2012)
9. National Research Council.: Oil in the Sea III: Inputs, Fates, and Effects. National Academies Press (US), Washington, DC, USA (2003)
10. Li, P., Cai, Q., Lin, W., Chen, B., Zhang, B.: Offshore oil spill response practices and emerging challenges. Mar. Pollut. Bull. **110**, 6–27 (2016)
11. Westerholm, D.A., Rauch, S.D., III, Kennedy, D.M., Basta, D.J.: Deepwater horizon oil spill: final programmatic damage assessment and restoration plan and final programmatic environmental impact statement. In: Natural Resources Science Plan 2011–2015. Springer, Berlin/Heidelberg, Germany (2011)
12. Piatt, J.F., Lensink, C.J., Butler, W., Nysewander, D.R.: Immediate impact of the 'Exxon Valdez' oil spill on marine birds. Auk **107**, 387–397 (1990)
13. Nevalainen, M., Helle, I., Vanhatalo, J.P.: Estimating the acute impacts of Arctic marine oil spills using expert elicitation. Mar. Pollut. Bull. **131**, 782–792 (2018)
14. Prabowo, A.R., Bae, D.M.: Environmental risk of maritime territory subjected to accidental phenomena: correlation of oil spill and ship grounding in the Exxon Valdez's case. Results Eng. **4**, 100035 (2019)
15. Amir-Heidari, P., Arneborg, L., Lindgren, J.F., Lindhe, A., Rosén, L., Raie, M., Axell, L., Hassellöv, I.-M.: A state-of-the-art model for spatial and stochastic oil spill risk assessment: a case study of oil spill from a shipwreck. Environ. Int. **126**, 309–320 (2019)
16. Grubesic, T.H., Nelson, J.R., Wei, R.: A strategic planning approach for protecting environmentally sensitive coastlines from oil spills: allocating response resources on a limited budget. Mar. Policy **108**, 103549 (2019)
17. Fan, C., Hsu, C.-J., Lin, J.-Y., Kuan, Y.-K., Yang, C.-C., Liu, J.-H., Yeh, J.-H.: Taiwan's legal framework for marine pollution control and responses to marine oil spills and its implementation on T.S. Taipei cargo shipwreck salvage. Mar. Pollut. Bull. **136**, 84–91 (2018)
18. Bullock, R.J., Perkins, R.A., Aggarwal, S.: In-situ burning with chemical herders for Arctic oil spill response: meta-analysis and review. Sci. Total Environ. **675**, 705–716 (2019)
19. Sardi, S.S., Qurban, M.A., Li, W., Kadinjappalli, K.P., Manikandan, K.P., Hariri, M.M., Al-Tawabini, B.S., Khalil, A.B., El-Askary, H.: Assessment of areas environmentally sensitive to oil spills in the western Arabian Gulf, Saudi Arabia, for planning and undertaking an effective response. Mar. Pollut. Bull. **150**, 110588 (2019)
20. Lenhard, R.J., Rayner, J.L., García-Rincón, J.: Testing an analytical model for predicting subsurface LNAPL distributions from current and historic fluid levels in monitoring wells: a preliminary test considering hysteresis. Water **11**, 2404 (2019). https://doi.org/10.3390/w11112404
21. US.EPA.: A decision-making framework for cleanup of sites impacted with light non-aqueous phase liquids (LNAPL). Us.Epa. 542-R-04-0, 86 (2005)
22. CRC CARE.: A practitioner's guide for the analysis, management and remediation of LNAPL cooperative research centre for contamination assessment and remediation of the environment, technical report series (2015)
23. Chevalier, L.R., Petersen, J.: Literature review of 2-D laboratory experiments in NAPL flow, transport, and remediation. Soil Sediment Contam. **8**, 149–167 (1999). https://doi.org/10.1080/10588339991339289
24. Saleem, M., Al-Suwaiyan, M.S., Aiban, S.A., Ishaq, A.M., Al-Malack, M.H., Hussain, M.: Estimation of spilled hydrocarbon volume—the state-of-the-art. Environ. Technol. **25**, 1077–1090 (2004). https://doi.org/10.1080/09593330.2004.9619401
25. Oostrom, M., Hofstee, C., Wietsma, T.W.: Behavior of a viscous LNAPL under variable water table conditions. Soil Sediment Contam. **15**, 543–564 (2006). https://doi.org/10.1080/15320380600958976

26. Oostrom, M., Dane, J.H., Wietsma, T.W.: A review of multidimensional, multifluid, intermediate-scale experiments: flow behavior, saturation imaging, and tracer detection and quantification. Vadose Zo. J. **6**, 610–637 (2007). https://doi.org/10.2136/vzj2006.0178
27. Zhao, S., Wang, J., Feng, S., Xiao, Z., Chen, C.: Effects of ecohydrological interfaces on migrations and transformations of pollutants: a critical review. Sci. Total Environ. **804**, 150140 (2022). https://doi.org/10.1016/j.scitotenv.2021.150140
28. Cavelan, A., Golfier, F., Colombano, S., Davarzani, H., Deparis, J., Faure, P.: A critical review of the influence of groundwater level fluctuations and temperature on LNAPL contaminations in the context of climate change. Sci. Total Environ. **806** (2022). https://doi.org/10.1016/j.scitotenv.2021.150412
29. Alazaiza, M.Y.D., Ngien, S.K., Bob, M.M., Kamaruddin, S.A., Ishak, W.M.F.: Non-aqueous phase liquids distribution in three-fluid phase systems in double-porosity soil media: experimental investigation using image analysis. Groundwater Sustain. Dev. **7**, 133–142 (2018). https://doi.org/10.1016/j.gsd.2018.04.002
30. Huang, Y., Wang, P., Fu, Z., Shen, H.: Experimental and numerical research on migration of LNAPL contaminants in fractured porous media. Hydrogeol. J. **28**, 1269–1284 (2020). https://doi.org/10.1007/s10040-020-02118-w
31. Badv, K., Mohammad Seyyedi, B., Nimtaj, A.: Numerical investigation of propagation of BTEX compounds in soil. Geotech. Geol. Eng. **38**, 3875–3890 (2020). https://doi.org/10.1007/s10706-020-01263-z
32. Foong, L.K., Rahman, N.A., Nazir, R., Sa'ari, R., Mustaffar, M.: Investigation of aqueous and non-aqueous phase liquid migration in double-porosity soil using digital image analysis. Chem. Eng. Trans. **63**, 685–690 (2018). https://doi.org/10.3303/CET1863115
33. Crawford, R.L., Alcock, J., Couvreur, J.F., Dunk, M., Fombarlet, C., Frieyro, O., Lethbridge, G., Mitchell, T., Molinari, M., Ruiz, H., Walden, T., Martin, D.E.: European oil industry guideline for risk-based assessment of contaminated sites (revised). CONCAWE Rep. (2003)
34. Alesse, B., Orlando, L., Palladini, L.: Non-invasive lab test in the monitoring of vadose zone contaminated by light non-aqueous phase liquid. Geophys. Prospect. **67**, 2161–2175 (2019). https://doi.org/10.1111/1365-2478.12809
35. Mercer, J.W., Cohen, R.M., Va, U.S.A.: Review Paper a Review of Immiscible Fluids in the Subsurface: Properties, Models, Characterization and Remediation [Nonaqueous phase liquids (NAPL's) have been discovered at numerous hazardous waste sites (e.g., Faust, 1985; Mercer et al., 19. J. Contam. Hydrol. 6, 107–163)] (1990)
36. Kacem, M., Esrael, D., Boeije, C.S., Benadda, B.: Multiphase flow model for NAPL infiltration in both the unsaturated and saturated zones. J. Environ. Eng. **145**, 04019072 (2019). https://doi.org/10.1061/(asce)ee.1943-7870.0001586
37. Azimi, R., Vaezihir, A., Lenhard, R.J., Majid Hassanizadeh, S.: Evaluation of LNAPL behavior in water table inter-fluctuate zone under groundwater drawdown condition. Water (Switzerland) **12** (2020). https://doi.org/10.3390/W12092337
38. Yang, Y.S., Li, P., Zhang, X., Li, M., Lu, Y., Xu, B., Yu, T.: Lab-based investigation of enhanced BTEX attenuation driven by groundwater table fluctuation. Chemosphere **169**, 678–684 (2017). https://doi.org/10.1016/j.chemosphere.2016.11.128
39. Charbeneau, R.: LNAPL Distribution and Recovery Model. Distribution and Recovery of Petroleum Hydrocarbon Liquids in Porous Media, vol. 1, p. 4760. API Publication (2007)
40. Jeong, J., Charbeneau, R.J.: An analytical model for predicting LNAPL distribution and recovery from multi-layered soils. J. Contam. Hydrol. **156**, 52–61 (2014). https://doi.org/10.1016/j.jconhyd.2013.09.008
41. Kechavarzi, C., Soga, K., Illangasekare, T.H.: Two-dimensional laboratory simulation of LNAPL infiltration and redistribution in the vadose zone (2005). J. Contam. Hydrol. **76**, 211–233 (2004). https://doi.org/10.1016/j.jconhyd
42. Kemblowski, M.W., Chiang, C.Y.: Hydrocarbon thickness fluctuations in monitoring wells. Groundwater **28**, 244–252 (1990). https://doi.org/10.1111/j.1745-6584.1990.tb02252.x
43. Lenhard, R.J., Johnson, T.G., Parker, J.C.: Experimental observations of nonaqueous phase liquid subsurface movement. J. Contam. Hydrol. **12**, 79–101 (1993). https://doi.org/10.1016/0169-7722(93)90016-L

44. Parker, J.C., Lenhard, R.J.: A model for hysteretic constitutive relations governing multiphase flow: 1. saturation-pressure relations. Water Resour. Res. **23**, 2187–2196 (1987). https://doi.org/10.1029/WR023i012p02187
45. Sookhak Lari, K., Johnston, C.D., Davis, G.B.: Gasoline multiphase and multicomponent partitioning in the vadose zone: dynamics and risk longevity. Vadose Zone J. **15**, 1–15
46. Van Geel, P.J., Sykes, J.F.: The importance of fluid entrapment, saturation hysteresis and residual saturations on the distribution of a lighter-than-water non-aqueous phase liquid in a variably saturated sand medium. J. Contam. Hydrol. **25**, 249–270 (1997). https://doi.org/10.1016/S0169-7722(96)00038-1
47. ITRC.: LNAPL site management: LCSM evolution, decision process, and remedial technologies. LNAPL-3. Interstate Technology & Regulatory Council, Washington, DC
48. Flores, G., Katsumi, T., Inui, T., Kamon, M.: A simplified image analysis method to study lnapl migration in porous media. Soils Found. **51**, 835–847 (2011). https://doi.org/10.3208/sandf.51.835
49. Ramli, M.H.: Dynamic Effects on Migration of Light Non-Aqueous Phase Liquids in Subsurface. Dissertation. Kyoto University (2014). https://doi.org/10.14989/doctor.k18487
50. Skoog, D.A., Holler, F.J., Crouch, S.R.: Principles of Instrumental Analysis. Thomsom Brooks/Cole, Belmont (2007)
51. Kechavarzi, C., Soga, K., Wiart, P.: Multispectral image analysis method to determine dynamic fluid saturation distribution in two-dimensional three-fluid phase two laboratory experiments. J. Contam. Hydrol. **46**(3–4), 265–293 (2000)
52. Flores, G., Katsumi, T., Eua-Apiwatch, S., Lautua, S., Inui, T.: Effects of repeated drainage and imbibition on the contamination behavior of a LNAPL and on its S-p relation. J. Geo-Eng. Sci. **3**, 15–30 (2016). https://doi.org/10.3233/jgs-150033
53. Flores, G., Katsumi, T., Inui, T., Ramli, H.: Characterization of LNAPL distribution in whole domains subject to precipitation by the simplified image analysis method. Coupled Phenom. Environ. Geotech. Theor. Exp. Res. Pract. Appl. Proc. Int. Symp. ISSMGE TC **215**, 573–577 (2013). https://doi.org/10.1201/b15004-76
54. Sudsaeng, S., Flores, G., Katsumi, T., Inui, T., Likitlersuang, S., Yimsiri, S.: Experimental study of diesel migration in P orous Media by Simplified Image Analysis Method. Geo-Environmental Engineering 2011 Kagawa National College of Technology, Takamatsu, Japan, May 21–22 2011
55. Flores, G., Tkatsumi, T., Inui, T., Takai, A.: Measurement of NAPL saturation distribution in whole domains by the simplified image analysis method. In: 18th International Conference on Soils Mechanics and Geotechnical Engineering (ICSMGE). Challenges Innov. Geotech. **4**, 3017–3020 (2013)
56. Flores, G., Katsumi, T., Eua-Apiwatch, S., Lautua, S., Inui, T.: Migration of different LNAPLs in subsurface under groundwater fluctuating conditions by the simplified image analysis method. J. Geo-Eng. Sci. **3**, 15–30 (2016). https://doi.org/10.3233/jgs-150033
57. Alazaiza, M.Y.D., Ramli, M.H., Copty, N.K., Ling, M.C.: Assessing the impact of water infiltration on LNAPL mobilization in sand column using simplified image analysis method. J. Contam. Hydrol. **238**, 103769 (2021). https://doi.org/10.1016/j.jconhyd.2021.103769
58. Alazaiza, M.Y.D., AI Maskari, T., Albahansawi, A., Amr, S.S.A., Abushammala, M.F.M., Aburas, M.: Diesel migration and distribution in capillary fringe using different spill volumes via image analysis. Fluids **6**, 1–11 (2021). https://doi.org/10.3390/fluids6050189
59. Alazaiza, M.Y.D., Ramli, M.H., Copty, N.K., Sheng, T.J., Aburas, M.M.: LNAPL saturation distribution under the influence of water table fluctuations using simplified image analysis method. Bull. Eng. Geol. Environ. **79**, 1543–1554 (2020). https://doi.org/10.1007/s10064-019-01655-3
60. Ramli, H., Flores, G.: The migration of LNAPL in subsurface affected by spill volume and precipitation. Int. Conf. Contam. Sites **2016**, 96–100 (2016)
61. Sudsaeng, S., Yimsiri, S., Flores, G., Katsumi, T., Inui, T., Likitlersuang, S.: Diesel migration in sand under groundwater movements. In: 5th Asia-Pacific Conference on Unsaturated Soils, vol. 2, pp. 493–498 (2012)

62. Yimsiri, S., Euaapiwatch, S., Flores, G., Katsumi, T., Likitlersuang, S.: Effects of water table fluctuation on diesel fuel migration in one-dimensional laboratory study. Eur. J. Environ. Civ. Eng. **22**, 359–385 (2018). https://doi.org/10.1080/19648189.2016.1197158
63. Ramli, H., Lee, Z.X., Azmi, M., Ahmad, F.: Capillary rise determination using simplified image analysis method. E3S Web of Conf. **195**, 03017 (2020). https://doi.org/10.1051/e3sconf/202019503017